

## Synthesis of Graphene oxide OG by recycling graphite from the rods of electrical storage devices: application to the retention of $Hg^{2+}$ in aquatic environments

M. Kadari<sup>1\*</sup>, M. Makhoulouf<sup>1</sup>, H. Soltani<sup>2</sup>, R. Rouighi<sup>2</sup>, M. Kaid<sup>2</sup>

<sup>1</sup> Fundamental and Apply Physics Laboratory FUNDAPL, Blida 1, Algeria

<sup>2</sup> Department of Chemistry, University D<sup>r</sup> Moulay Taher, Saida, Algeria

\*Corresponding author: mohamed\_msma@yahoo.fr; Tel.: +213 24 33 09 92; Fax: +21300 00 00

### ARTICLE INFO

#### Article History :

Received : 21/01/2021

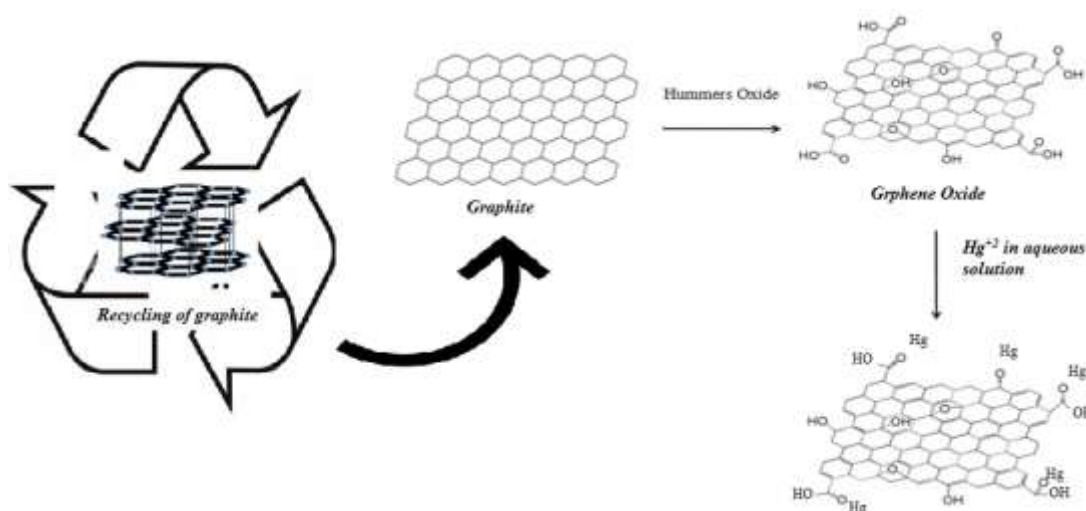
Accepted : 17/07/2021

#### Key Words:

Graphene Oxide;  
Hummer method;  
Mercuric ions;  
Recycling graphite.

### ABSTRACT/RESUME

**Abstract:** Seen the important utility of Graphene Oxide (OG) in various fields; This prestigious material has been synthesized by following the hummer method modified by recycling graphite rods from electrical storage devices and characterized by different characterization methods such as: Fourier transform infrared spectroscopy (FTIR), X-ray diffraction (DRX), and scanning electron microscope (SEM) to be able to see the structure and morphology of the synthesized material. The study of the elimination of mercuric ions ( $Hg^{2+}$ ) by OG was verified by a parametric, a thermodynamic and a kinetic study. The results showed that this adsorption is exothermic, spontaneous with an order between the adsorbent and the adsorbate and that the adsorption process follows the Langmuir model with pseudo-second-order kinetics. The best yield in this study was 75 % under the optimal conditions.



## **I. Introduction**

In recent years, climate change, the growth of the human population and the insufficiency of water resources have made the rehabilitation of polluted water an urgent necessity [1], [2]. To this end, the protection of the environment has become a major concern of our society, thus encouraging the development of processes for the improvement of pollution control methods.

Mercury is a heavy metal found in nature in different chemical forms. It is a shiny silvery metal and it is the only one which presents in liquid form under normal conditions of temperature and pressure without super cooling phenomenon [3], [4], conditions in which it has a significant vapor pressure because beyond that, it vaporizes easily.

Mercury has eight natural isotopes: seven stable, with mass numbers 204, 202, 201, 200, 199, 198, 196 and a secondary radioactive with mass number 194 [5]. Mercury is present in water either in divalent form complexed by organic species or not complexed, these two forms are the most frequently encountered.

Several depollution methods and techniques have been developed in order to conserve the planet, the environment and living beings. Among these techniques, chemical precipitation processes [6], [7], ion exchange [8], electrolysis [9], membrane processes and adsorption [10], [11].

Adsorption is one of the processes that has shown great profitability for removing different types of contaminants [12]. In addition, the research and development of new effective, ecological, profitable and economical adsorbents for water treatment is a great challenge [13].

Graphene oxide is a very popular material with great potential for its application in various fields of research [14] such as adsorption of metal cations [15]. Graphene oxide (GO) is a synthetic material made from one of the allotropic forms of carbon called graphite [16], it is formed from a single layer of graphite therefore which can be considered as a single mono-molecular layer of graphene containing different oxygen functional groups such as epoxides (C-O-C), carbonyl (C=O), alcohols (-OH) and carboxylic acids (O-C=O).

In this work, we were interested in: Firstly the synthesis of graphene oxide by recycling graphite rods from electrical storage devices [17]. Second to the study of the fixation of mercuric ions on the mono-molecular layer of graphene oxide OG in aquatic environments. To this end, a parametric study, a thermodynamic study and a kinetic study were made to fully understand the process of this phenomenon.

## **II. Materials and methods**

Graphene oxide was synthesized by modified Hummer method. For this purpose, chemical oxidation of graphite by recycling graphite rods from electrical storage devices gives us graphite oxide and the exfoliation of the latter gives rise to the obtention of the nano-sheets of graphene oxide (OG) [17]–[19].

2 g of graphite and 1 g of sodium nitrate  $\text{NaNO}_3$  were mixed with 46 ml of the sulfuric acid  $\text{H}_2\text{SO}_4$  and stirred in an ice bath for 60 min. Then, under vigorous agitation, 6 g of  $\text{KMnO}_4$  were slowly added, so that the temperature of the mixture remains below 5 °C. After a 2 hours agitation of the solution at a temperature of 35 °C, 30 ml of distilled water was slowly added, giving an exothermic reaction allowing the solution to reach a temperature of 95°C [17].

The solution has been diluted with a large amount of distilled water (75 ml) and treated with a hydrogen peroxide solution ( $\text{H}_2\text{O}_2$ , 30%) to reduce the residual permanganate to soluble manganese ions until the gas release ceases.

Finally, the graphite oxide solution was subjected to an ultrasonic treatment for 30 minutes in order to exfoliate the sheets of graphite oxide and obtain the graphene oxide (OG), the latter was centrifuged and washed by a solution of HCl (37%) then by distilled water (several times). Graphene oxide was dried for 24 h at 60 °C.

### **II.1. Experimental**

Our sample has been characterized on a brand name FTIR-ATR spectrometer (Alpha-Brucker), in the field of medium infrared wave numbers, between 400 and 4000  $\text{cm}^{-1}$ . This device is controlled by Opus 6.5 software, and equipped with a Total Reflectance Accessory (ATR) made of robust diamond crystal designed to facilitate meaningful analysis without the use of KBr pellets.

X-ray diffraction is based on the recording of a diffractogram, which makes it possible to identify / quantify the phases, to calculate the crystallographic parameters and to determine the average size of the crystallites by different methods (Scherrer, Williamson-Hall). Our sample was analyzed using a D8 Advance Eco Diffractogram (Bruker) operating with a copper tube ( $\lambda = 1.54 \text{ \AA}$ ). The analysis by scanning electron microscope (SEM) was made to see the morphology and the structural characteristics of the "nano-composite samples. In order to verify our studied material, and to better observe the morphology of our samples we used an SEM type Quanta FFG 250.

### III. Results and discussion

The analysis of OG by Fourier Transform Infra-Red spectroscopy FTIR-ATR; shows the main chemical functions. A broad band at around  $3039\text{ cm}^{-1}$  assigned to hydroxyl groups O-H and water molecules  $\text{H}_2\text{O}$  [20], A large peak in the form of a doublet, one around  $1566\text{ cm}^{-1}$  attributed to  $\text{C}=\text{C}$  bonds and the other around  $1637\text{ cm}^{-1}$  is more often attributed to  $\text{C}=\text{O}$  group (Figure 1).

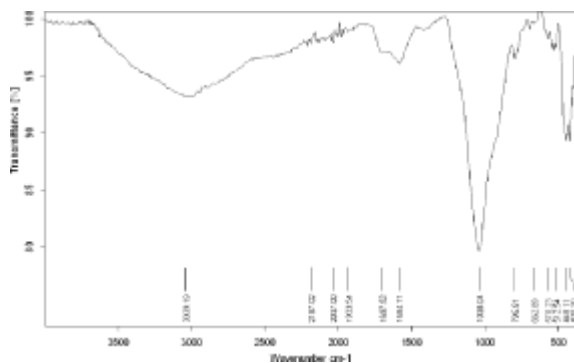


**Figure 1.** Infrared spectra of Graphene oxide.

X-ray diffraction analysis was used to determine interatomic distances and the arrangement of atoms in crystal networks. The total chemical exfoliation of graphene nano-sheets was confirmed by X-ray diffraction (DRX). The X-ray spectra of graphite powder (Figure 2) show the hexagonal structure according to orientation (002), as was revealed by the single peak at  $2\theta = 25^\circ$  which corresponds to a spacing of about  $3.4\text{ \AA}$  between the graphite planes.

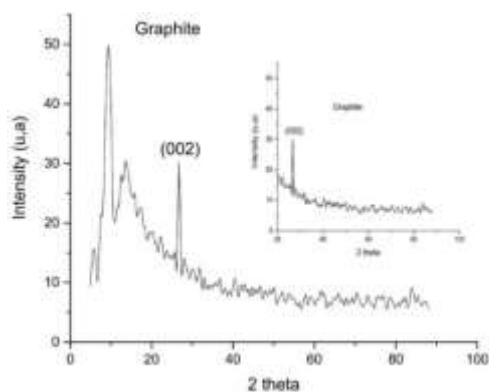


**Figure 2.** X-ray diffraction of graphite.

The X-ray spectra of Graphene Oxide (OG) (Figure 3), show the absence of peak diffraction compared to graphite ( $2^\theta = 26.4^\circ$ ), this indicates the removal of the periodicity in the structure of the exfoliated Graphene [21], [22].

In fact, the increase in the intercalary spacing following the oxidation of graphite comes from the intercalation of oxygen-containing groups between the layers of graphite, thus weakening the Van Der Waals forces between the layers, which allows an easy exfoliation via sonication in aqueous solution.

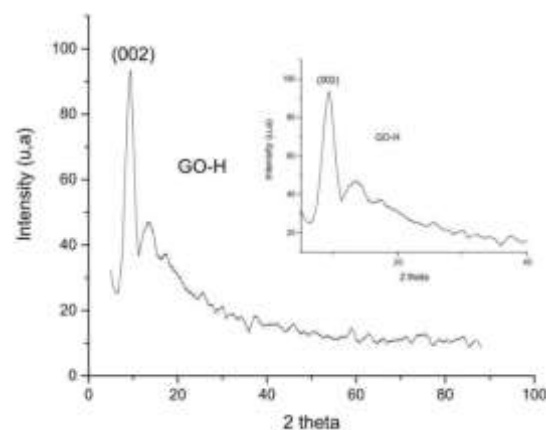


**Figure 3.** X-ray diffraction of Graphene oxide.

The scanning electron microscope (SEM) allows to surface images, virtually all solid materials. It is one of the most widely available instruments for studying and analyzing the structural characteristics of nano-composites at the micrometric scale [23]. The (Figure 4) shows the enlargement of the graphite grains. This scan electron microscopy image shows a more homogeneous expansion on the crushed sample. From the (Figure 5), we can see that the images of our products show the dynamic form of graphene oxide OG and confirm the existence of homogeneity in the microscopic structure.

### IV. Parametric study

In this work, we chose molecular absorption spectroscopy with 2-[5-(2-Hydroxy-5-sulfophenyl)-3-phenyl-1-formazyl] benzoic acid, known as Zincon. The latter is particularly appropriate for the determination of mercuric ions and some other elements by UV-visible.

For this purpose, a spectrophotometer UV-2401PC of Shimadzu mark was used for the analysis of the concentration of cations metallic. The  $\text{Hg}^{+2}$  calibration was performed with standard solutions with concentrations ranging from  $5.10^{-4}$  to  $10^{-3}$  mol/l. The calibration curves (absorbance according to concentration) obtained from the linear regression of experimental points showed good

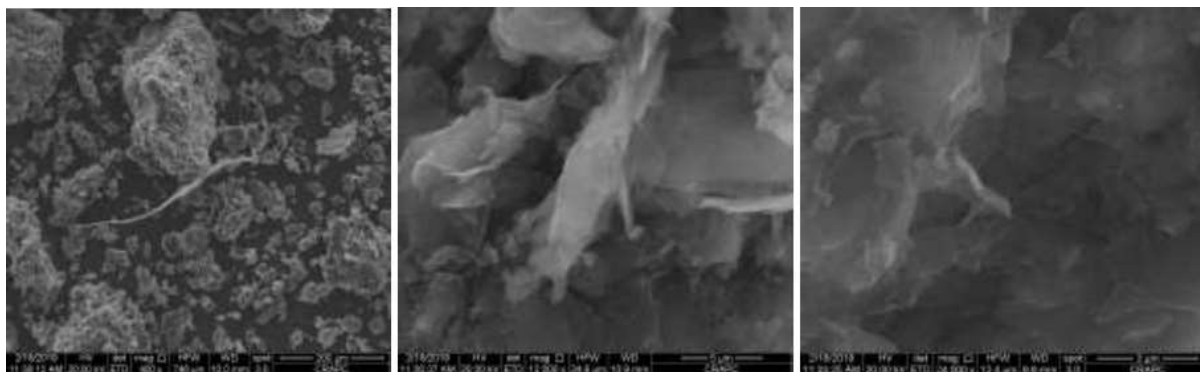


Figure 4. SEM images of graphite

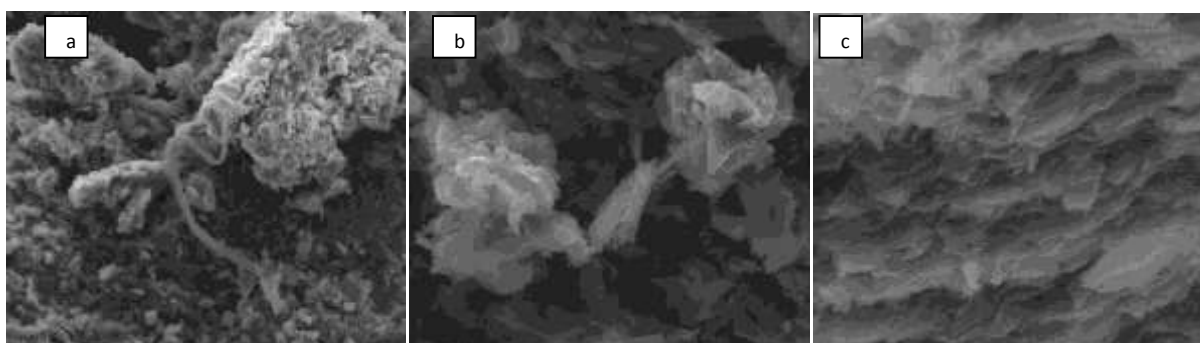


Figure 5. SEM images of Graphene Oxide

linearity with a wavelength of  $620 \text{ cm}^{-1}$ . The regression coefficient is 0.987.

#### IV.1. Equilibrium time

Since the adsorption phenomenon is a phenomenon of fixation of the metal cations on the external layer of the adsorbent, the time required for this fixation plays a very important role in this study [24].

To this end, the study of this parameter was carried out at times ranging from 0 to 50 minutes with an adsorbent mass of 0.1 g and the results are shown in the figure (Figure 6).

Based on these results, we can say that the adsorption of mercuric ions reached a maximum just after 10 minutes, after this time the extraction yield will probably decrease due to the effect of the agitation [25].

#### IV.2. Effect of initial concentration of $\text{Hg}^{+2}$

For this reason, several concentrations have been prepared in volumetric flasks  $10^{-4}$ ,  $2.10^{-4}$  and  $5.10^{-4}$  M and each mixed with the same mass of the prepared GO under medium stirring [26].

At equilibrium, the mixtures are separated by centrifugation and the supernatant of the solutions

was determined by UV-visible spectrometry. The results are shown in the figure (Figure 6).

The results give us the impression that more the concentration of metal ions increases, more the extraction efficiency decreases and this may be due to the repulsive effect between the cations and the saturation of the sites.

#### IV.3. Effect of the amount of the OG

In order to find a better Adsorbent/adsorbate ratio for this extraction, we prepared three solutions of the same concentration  $10^{-4}$  M and mixed each with different amounts of Graphene oxide OG 0.05 g, 0.1 g and 0.2 g. In the same way as the previous step, we have determined the concentrations of mercuric ions remaining in solutions. Figure (Figure 6) shows the effect of the amount of adsorbent on the extraction yield of  $\text{Hg}^{+2}$ .

The results shown in Figure 6, confirms the results obtained in the study of the effect of the concentration of the pollutant. Which means that the more the quantity increases, the more the extraction yield increases.

The quantity of support of 0.1 g of our adsorbent seems to be the best mass, which gave us a better extraction yield (73 %).

#### IV.4. pH Effect

The pH effect is a very important parameter for the adsorption process of mercuric ions  $Hg^{2+}$  on our material and for this a solution of nitric acid  $HNO_3$  was added to the solution studied to adjust the different pH (3.5 – 4.5 and 5.8) Figure 6.

The best extraction yield obtained is pH = 5.8, this is due to the stability of GO in basic media than in acidic media which gave us a pasty form.

#### IV.5. Effect of the addition of salts

The study of the effect of salt on mercury extraction was carried out by varying the concentration of  $NaNO_3$  (0.01, 0.1 and 1M) added in solution which contains the metal cations and the results are shown in Figure 6.

The increase in the concentration of salts in solution plays the role of inhibitor for the fixation of mercuric ions on the outer layer of our material; this is explained by the competition of the common ion released by the  $NaNO_3$  salt in solution.

#### IV.6. Effect of temperature

For this parameter, we have varied the temperature at which our extraction was made (25, 35, 40 and 50 °C) and as was expected, the rise in temperature inevitably leads to a decrease in the extraction yield, which leaves us to say, as a first result, that our adsorption is exothermic Figure 6.

#### V. Thermodynamic study

The determination of the thermodynamic parameters ( $\Delta H$ ,  $\Delta S$  and  $\Delta G$ ) of the extraction of mercury ions was studied using the following thermodynamic relationships [27], [28]:

$$\Delta G^\circ = \Delta H^\circ - T\Delta S^\circ \quad (01)$$

$$\ln \Delta G^\circ = -RT \ln K_d \quad (02)$$

From these two equations, we get the following expression:

$$\ln K_d = \frac{\Delta S^\circ}{R} - \frac{\Delta H^\circ}{RT} \quad (03)$$

The calculation of certain thermodynamic parameters is essential to determine the nature of the retention process. The equilibrium constant  $K_d$  can be calculated from the following relation:

$$K_d = \frac{q_e \left( \frac{m}{v} \right)}{[C_0 - q_e \frac{m}{v}]} \quad (04)$$

The adsorption capacity ( $q$ ) of the metal ion studied by graphene oxide is determined by the following relationship:

$$q_e \left( \frac{mg}{g} \right) = \frac{(C_0 - C_e) \cdot V \cdot M}{m} \quad (05)$$

$q_e$  : Sorption capacity at equilibrium

$C_0$  and  $C_e$  : Are the concentrations of  $Hg^{2+}$  at the initial state and at equilibrium respectively

$V$  : Volume of the treated mercury solution (10 ml)

$M$  : Molar mass of ( $Hg(NO_3)_2$ ,  $H_2O$ )

$m$  : Mass of the Graphene Oxide OG

$R$  : Ideal gas constant ( $R = 8,314 J \cdot mol^{-1} \cdot K^{-1}$ )

$K_d$  : Distribution coefficient of  $Hg^{2+}$  between the two phases, aqueous and solid

The thermodynamic parameters are listed in Table 1, where  $\Delta G$  values were obtained by plotting  $\ln K_d$  as a function of  $1/T$  (Figure 7).

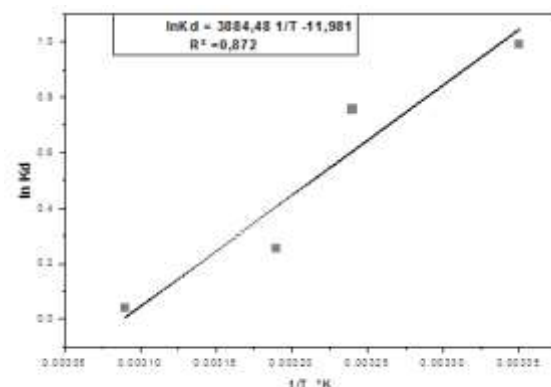


Figure 7. Evolution of  $\ln K_d$  as a function of  $1/T$ .

The results of the thermodynamic study showed that this adsorption is exothermic, spontaneous with an order between the adsorbent and the adsorbate.

#### VI. Adsorption isotherm

The study of the adsorption isotherm is fundamental and plays an important role in determining the maximum adsorption capacity. In order to adapt to the system considered, an adequate model being able to reproduce the experimental results obtained, the models of Langmuir and Freundlich were considered.

$\Delta H^\circ$ (Kcal/mol)	$\Delta S^\circ$ (Cal /mol .K)	$\Delta G^\circ$ (Kcal/mol)
- 7.72	- 23.6	- 0.67

Table 1. Thermodynamic study

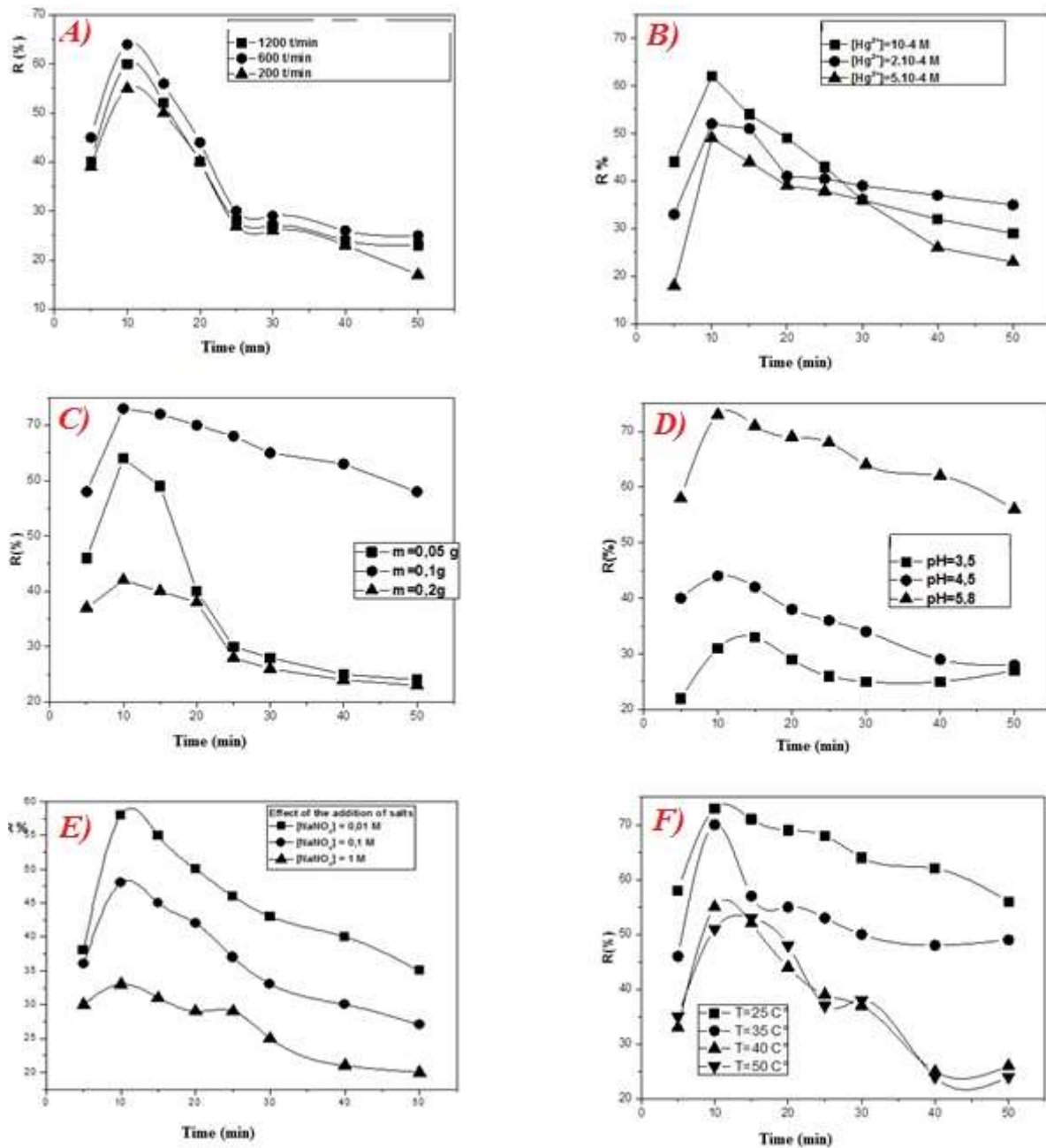


Figure 6. A) Equilibrium time, B) Effect of initial concentration of  $Hg^{+2}$ , C) Effect of the amount of the OG, D) Effect of pH, E) Effect of the addition of salts, F) Effect of temperature

These two models are the most used to adjust the adsorption of heavy metals (Figure 8).

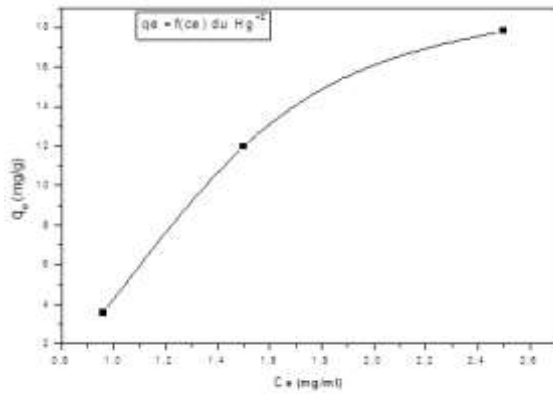


Figure 8. Adsorption Isotherm of  $Hg^{+2}$

In the figure, the quantities adsorbed as a function of the concentrations of the aqueous solution in equilibrium show that the isotherm is type 1. This behavior is encountered in the case where the adsorption of the solvent is weak, and when the molecules are not oriented vertically, but rather flat.

### VI.1. Langmuir isotherm

The Langmuir isotherm is related to the adsorption of metal adsorbates on a surface containing a defined number of sites or linking groups. Mathematically, the Langmuir isotherm model is defined by the following equation:

$$\frac{1}{q_e} = \frac{1}{q_m \cdot K_L \cdot C_e} + \frac{1}{q_m} \quad (06)$$

Or

$Q_m$  is the monolayer capacity of the adsorbent and  $K_L$  is the Langmuir adsorption constant.  $q_m$  and  $K_L$  can be determined from the slope and the y-intercept, respectively by plotting  $1/q_e$  with respect to  $1/C_e$  (Figure 9)

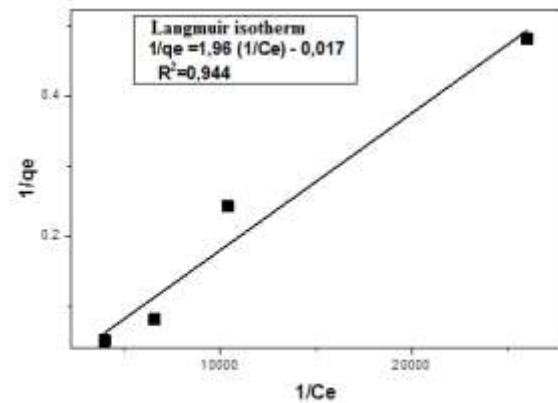


Figure 9. Langmuir isotherm

### VI.2. Freundlich isotherm

This model describes systems where the adsorption takes place on heterogeneous surfaces with interactions between the adsorbed molecules; the linear form is given by the following equation:

$$\log q_e = \log K_f + 1/n \log C_e \quad (07)$$

The constant ( $K_f$ ), due to the binding energy, and the heterogeneity factor ( $1/n$ ) which measures the deviation from the linear part are determined from a  $\log q_e$  curve as a function of  $\log C_e$ . The experimental results obtained at room temperature are presented in Figure 10.

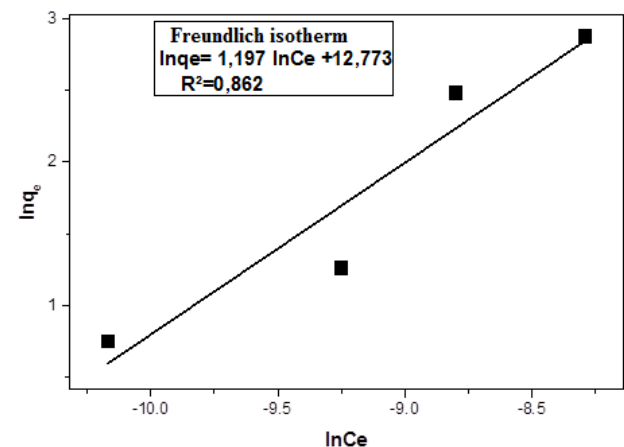


Figure 10. Freundlich isotherm

The adsorption data obtained show that the adsorption of  $Hg^{2+}$  by OG follows the Langmuir model.

VII. Kinetic study

VII.1. Pseudo first order kinetics

In this model (model of the Lagergren equation), it is assumed that the sorption rate at time t is proportional to the difference between the quantity adsorbed at equilibrium (qe) and the quantity (qt) adsorbed at this instant and that the adsorption can be reversible. The speed law is written :

$$\ln(q_e - q_t) = \ln(q_e) - k_1t \tag{08}$$

The pseudo first order kinetic model represents the relationship between the difference between the equilibrium retention capacity and the retention capacity less than the equilibrium time and the stirring time of the extractant [27]–[29].

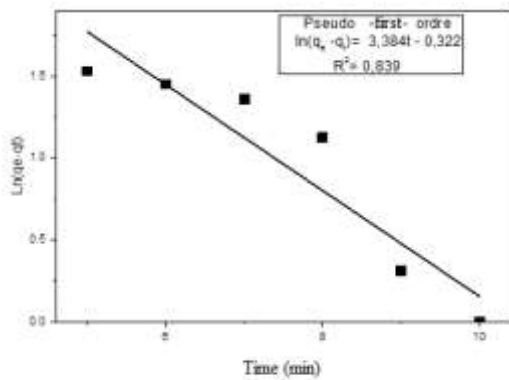


Figure 11. Pseudo-first-order

In other words, the sorption is all the faster as the system is far from equilibrium. The curve  $\ln(q_e - q_t)$  as a function of the stirring time is shown in Figure 11.

VII.2. Pseudo second order kinetics

The kinetic model of the pseudo second order has for mathematical equation the following linear relation:

$$\frac{1}{qt} = \frac{1}{qe^2 \cdot K} + \frac{1}{qt} \tag{09}$$

The pseudo second order kinetic model represents the relationship between the stirring time and the retention capacity at this time, less than the equilibrium time, and the contact time between the extractant and the mercury. The curve of  $t / q_t$  as a function of t is presented in Figure 12.

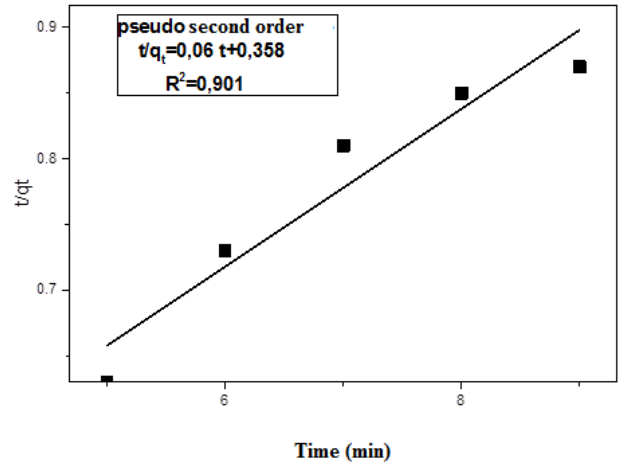


Figure 12. Pseudo second order

The figure shows that the experimental results obtained perfectly follow the linear variation given by the representative equation of pseudo second order kinetics.

VIII. Conclusion

The aim of this work was to carry out a study of the adsorption of mercuric ions  $Hg^{+2}$  existing in aquatic environments by an adsorbent not expensive, by recycling the raw material (graphite). The results obtained were encouraging in this study thanks to the low cost of our material and the elimination percentage, which reached 75%.

Our study has shown us that the adsorption process in this study is exothermic, spontaneous with an order between the solid phase and the liquid phase and the isotherm follows the Langmuir model with pseudo second order kinetics.

This study has given us perspectives with regard to the elimination of existing metal cations in aquatic environments by graphene oxides synthesized by recycling.

IX. References

1. Abedin, Md. A.; Collins, A. E.; Habiba, U.; Shaw, R. Climate Change, Water Scarcity, and Health Adaptation in Southwestern Coastal Bangladesh ; *International Journal of Disaster Risk Science*; 10 (2019) 28-42
2. Kundzewicz, Z. W.; Döll, P. Will groundwater ease freshwater stress under climate change? ; *Hydrological Sciences Journal*; 54 (2009) 665-675
3. Aastrup, M.; Johnson, J.; Bringmark, E.; Bringmark, I.; Iverfeldt, Å. Occurrence and transport of mercury within a small catchment area ; *Water, Air, and Soil Pollution*; 56 (1991) 155-167
4. Berg, T.; Aspö, K.; Steinnes, E. Transport of Hg from Atmospheric mercury depletion events to the mainland of Norway and its possible influence on Hg deposition ; *Geophysical Research Letters*.; 35 (2008) L09802
5. Ryan, F.; Lepak, Runsheng, Y.; David, P.; Krabbenhoft; Jacob, M.; Ogorek; John, F.; DeWild; Thomas, M.; Holsen; James, P.;



- Hurley. Use of Stable Isotope Signatures to Determine Mercury Sources in the Great Lakes , *Environmental Science & Technology Letters*; 2 (2015) 335-341.
6. Herva, J.; Meskus, E. Upgrading the Chemical Precipitation Process Using a Fixed Film Biological Reactor: A Case Study of the Taskila Plant of Oulu, Finland ; *Chemical Water and Wastewater Treatment*; (1998) 255-265.
  7. Wang, F.; Yu, X.; Maofa, Ge.; Sujun, Wu.; Guan, J.; Tang, J.; Xiao, W.; Robert, O.; Ritchie .Facile self-assembly synthesis of  $\gamma$ -Fe<sub>2</sub>O<sub>3</sub> /graphene oxide for enhanced photo-Fenton reaction , *Environmental Pollution* , 248 (2019) 229-237.
  8. Soldatov, V. S.; Elinson, I. S.; Shunkevich, A. A.; Pawlowski, L.; Wasag, H. Air Pollution Control with Fibrous Ion Exchangers , *Chemistry for the Protection of the Environment* (1996) 55-66.
  9. Drogui, P.; Elmaleh, S.; Rumeau, M.; Bernard, C.; Rambaud, A. Hydrogen peroxide production by water electrolysis: Application to disinfection, *Journal of Applied Electrochemistry*, 31 (2001) 877-882
  10. Ritter, J. A.; Ebner, A. D. State-of-the-Art Adsorption and Membrane Separation Processes for Hydrogen Production in the Chemical and Petrochemical Industries , *Separation Science and Technology*, 42 (2007) 1123-1193
  11. Zahoor, M.; Mahramanlioglu, M. Removal of Phenolic Substances from Water by Adsorption and Adsorption-Ultrafiltration , *Separation Science and Technology*, 46 (2011) 1482-1494.
  12. Kadari, M.; Kaid, M.; Ben Ali, M.; Villemin, D. Selective study of elimination of Cd (II) and Pb (II) from aqueous solution by novel hybrid material , *Journal of the Chinese Advanced Materials Society*, 5 (2017) 149-157
  13. Khan, S. J.; Murchland, D.; Rhodes, M.; Waite, T. D. Management of Concentrated Waste Streams from High-Pressure Membrane Water Treatment Systems , *Critical Reviews in Environmental Science and Technology*, 39 (2009) 367-415.
  14. Grajek, H.; Witkiewicz, J, Jonik.; Wawer, T.; Purchala, M. Applications of Graphene and Its Derivatives in Chemical Analysis , *Critical Reviews in Analytical Chemistry*, 50 (2020) 445-471
  15. Ma, Y.; Kou, Y.; Jin, S.; Shao, W.; Li, X. Adsorption of Hg(II) in aqueous solution by magnetic graphene oxide grafted polymaleicamide dendrimer nanohybrids , *Separation Science and Technology*, 54 (2019) 2409-2417.
  16. Naz, A.; Kausar, A.; Siddiq, M. Influence of Graphite Filler on Physicochemical Characteristics of Polymer/Graphite Composites: A Review , *Polymer-Plastics Technology and Engineering*, 55 (2016) 604-625.
  17. Hummers, W. S.; Offeman, R. E. Preparation of Graphitic Oxide , *Journal of the American Chemical Society*, 80 (1958) 1339-1339.
  18. Shao, G.; Lu, Y.; Wu, F.; Yang, C.; Zeng, F.; Wu, Q. Graphene oxide: the mechanisms of oxidation and exfoliation , *Journal of Materials Science*, 47 (2012) 4400-4409
  19. Stankovich, S.; Dikin, D.; Piner, D.; Kohlhaas, A.; Kleinhammes, A.; Yuanyuan, J.; Wu, Y.; Nguyen, T.; Ruoff, S. Synthesis of graphene-based nanosheets via chemical reduction of exfoliated graphite oxide , *Carbon*, 45 (2007) 1558-1565
  20. Chua, K.; Sofer, Z.; Pumera, M. Graphite Oxides: Effects of Permanganate and Chlorate Oxidants on the Oxygen Composition , *Chemistry - A European Journal*, 18 (2012) 13453-13459
  21. Fachina, J.; de Andrade, B.; Guerra, S.; dos Santos, T.; Bergamasco, R.; Vieira, S. Graphene oxide functionalized with cobalt ferrites applied to the removal of bisphenol A: ionic study, reuse capacity and desorption kinetics , *Environmental Technology*, (2020) 1-17
  22. Phatthanakittiphong, T.; Seo, G. Characteristic Evaluation of Graphene Oxide for Bisphenol A Adsorption in Aqueous Solution , *Nanomaterials*, 6 (2016) 128
  23. Huang, X.; Qi, X.; Boey, F.; Zhang, H. Graphene-based composites », *Chemical Society Reviews*., 41 (2012) 666-686
  24. Kadari, M.; Kaid, M.; Ben Ali, M.; Villemin, D. The intercalation of Zn/Al-HDL by the diamino-dodecylphosphonic acid: synthesis and properties of adsorption of basic fuchsin , *Journal of the Chinese Advanced Materials Society*, 4 (2016) 148-157
  25. Goswami, A.; Purkait, M. Kinetic and Equilibrium Study for the Fluoride Adsorption using Pyrophyllite , *Separation Science and Technology*, 46 (2011) 1797-1807
  26. Kara, A.; Demirbel, E. Physicochemical Parameters of Cu(II) Ions Adsorption from Aqueous Solution by Magnetic-Poly(divinylbenzene-n-vinylimidazole) Microbeads , *Separation Science and Technology*, 47 (2012) 709-722
  27. Emami, A.; Rahbar-Kelishami, A. Zinc and nickel adsorption onto a low-cost mineral adsorbent: kinetic, isotherm, and thermodynamic studies , *Desalination and Water Treatment*, 57 (2016) 21881-21892
  28. Kamari, A.; Ngah, W. Adsorption of Cu(II) and Cr(VI) onto Treated *Shorea dasyphylla* Bark: Isotherm, Kinetics, and Thermodynamic Studies , *Separation Science and Technology*, 45 (2010) 486-496.
  29. Yousef, A.; Morsy, A.; Hagag, S. Uranium ions adsorption from acid leach liquor using acid cured phosphate rock: kinetic, equilibrium, and thermodynamic studies , *Separation Science and Technology*, 55 (2020) 648-657.

**Please cite this Article as:**

Kadari M., Makhlouf M., Soltani H., Rouighi R., Kaid M., Synthesis of Graphene oxide OG by recycling graphite from the rods of electrical storage devices: application to the retention of Hg<sup>2+</sup> in aquatic environments, *Algerian J. Env. Sc. Technology*, 9:2 (2023) 3061-3069